

# Scattering and Swelling Properties of Inhomogeneous Polyacrylamide Gels

Simon Mallam,<sup>†</sup> Ferenc Horkay,<sup>‡</sup> Anne-Marie Hecht,<sup>†</sup> and Erik Geissler<sup>\*,†,§</sup>

Laboratoire de Spectrométrie Physique,<sup>§</sup> Université de Grenoble I, B.P. 87, F-38402 St. Martin d'Hères Cedex, France, and Department of Colloid Science, Loránd Eötvös University, H-1088 Budapest VIII, Puskin u. 11-13, Hungary.

Received October 11, 1988; Revised Manuscript Received January 30, 1989

**ABSTRACT:** An investigation is described of a set of chemically cross-linked polyacrylamide hydrogels prepared by copolymerization of acrylamide in presence of different amounts of bisacrylamide. These networks were studied by using osmotic and mechanical measurements, dynamic light scattering, and small-angle X-ray scattering (SAXS) techniques. The form of the concentration dependence of the swelling pressure was found to vary with the cross-linking density, water being a good solvent for the loosely cross-linked gels, while at higher bisacrylamide content the solvent power diminishes. The ratio of the longitudinal osmotic modulus obtained from mechanical and osmotic observations to that from dynamic light scattering was found to increase with increasing cross-linking, in agreement with SAXS observations of the amplitude of the concentration fluctuations associated with the static heterogeneities in the sample. Furthermore, for all the gels studied, the values of the correlation lengths determined by three independent methods—SAXS, dynamic light scattering intensity, and collective diffusion coefficient measurements—were consistent with each other.

## Introduction

In a previous article,<sup>1</sup> a comparison between dynamic light scattering and osmotic swelling pressure measurements was reported for a set of polyacrylamide water gels, copolymerized lightly with the cross-linking agent *N,N'*-methylenebisacrylamide. This comparison served as a calibration for the observations of the intensity of the dynamic light scattering signal. It was noted that in the presence of structural heterogeneities involving local variations in the mean concentration of the gel, significant deviations could be expected between the values of the longitudinal osmotic modulus  $M_{os} = K_{os} + 4G_s/3$  in the two types of experiment, where  $K_{os}$  is the compressional osmotic modulus and  $G_s$  the shear modulus of the swollen network. In particular, it was found that the ratio of the moduli from these two experiments could, with certain simplifying assumptions, be related to the mean-square amplitude of the static concentration fluctuations in the network,  $\langle \Delta c^2 \rangle$ . This latter quantity has a counterpart in small-angle X-ray scattering (SAXS).

In this article we report results of dynamic light scattering, osmotic swelling pressure, and mechanical measurements, as well as static light scattering and SAXS, upon a set of polyacrylamide gels swollen to equilibrium, in which the degree of heterogeneity was varied by changing the extent of cross-linking. The poly(acrylamide/bisacrylamide) system investigated displays a qualitative change of aspect with increasing cross-linking density. The gels are transparent and flexible at low bisacrylamide content, becoming opaque and fragile at high cross-linking density. A previous investigation, performed on similar gels at their concentration of preparation,<sup>2</sup> showed that during the formation of the network, structural heterogeneities develop having characteristic lengths lying in the range 50–2500 Å.

One of the objects of the present investigation is to examine how these heterogeneities influence the osmotic and elastic properties of the networks. The results of the osmotic swelling and light scattering measurements are compared with those of SAXS. In addition, observations are reported of the behavior of the various moduli,  $K_{os}$ ,  $M_{os}$ ,  $G_s$ , and the volume elastic modulus,  $G_v$ .

## Theoretical Background

In a swollen network at polymer concentration  $c$ , the swelling pressure  $\omega$  is defined by the difference between the osmotic pressure  $\Pi$  tending to swell the gel and a restraining elastic component  $G_v$  (volume elastic modulus), such that

$$\omega = \Pi(c) - G_v(c) \quad (1)$$

At swelling equilibrium with the pure diluent at concentration  $c = c_e$ , the two terms on the right-hand side of eq 1 cancel, giving  $\omega = 0$ .  $\Pi$  can be represented by a power series<sup>3</sup> in  $c$ , each successive term of which corresponds to a higher order interaction between the polymer molecules. As a result of correlations between monomers in good solvent conditions,<sup>4</sup> however, the dominant term adopts the nonintegral power form

$$\Pi = Ac^{9/4} \quad (2)$$

At the  $\Theta$  condition, the second-order coefficient  $A = 0$ , and the right-hand side of eq 2 starts with a third-order term,  $A_3c^3$ . Although it is conceivable to devise an interpolation expression for the region intermediate between the good solvent and  $\Theta$  regimes,<sup>5</sup> it will be sufficient for the present purpose to replace (2) by

$$\Pi = Ac^s \quad (3)$$

with

$$s = 3\nu/(3\nu - 1)$$

in which  $\nu$ , the excluded-volume exponent, takes a value close to  $3/5$  for excluded-volume conditions in the asymptotic semidilute region and  $1/2$  in  $\Theta$  conditions.<sup>4</sup>

The elastic term in eq 1 can be written

$$G_v(c) = G_v^*(c/c_e)^m \quad (4)$$

in which  $G_v^*$  is the value of  $G_v$  at swelling equilibrium, and the theoretically expected value<sup>6,7</sup> of the exponent  $m$  is  $1/3$ . According to ref 6 and 7, the volume elastic modulus  $G_v$ , describing isotropic deformations of the network, is simply equal to the shear modulus  $G_s$  that describes network deformations at constant volume.

Fitting the swelling pressure measurements to eq 1 allows the osmotic compressional modulus,  $K_{os} = (c\partial\omega/\partial c)$ , to be calculated. In gels that display static spatial varia-

<sup>†</sup> Université de Grenoble I.

<sup>‡</sup> Loránd Eötvös University.

<sup>§</sup> CNRS associate laboratory.

**Table I**  
**Dynamic Light Scattering Characteristics of the Polyacrylamide Samples**

sample	$c_e$ , g/cm <sup>3</sup>	$(\partial\epsilon/\partial c)^2$ , <sup>a</sup> cm <sup>6</sup> /g <sup>2</sup>	$\Gamma$ , <sup>b</sup> s <sup>-1</sup> /10 <sup>-4</sup>	$\mu_2/\Gamma^{2c}$
8/1	0.0465	0.225	2.3 ± 0.2	0.07
8/2	0.0618	0.221	2.4 ± 0.2	0.02
8/3	0.0746	0.217	3.0 ± 0.2	0.04
8/4	0.0843	0.216	2.6 ± 0.4	0.12
8/5	0.0861	0.215		

<sup>a</sup> Calculated from  $\epsilon = n^2$ , where  $n$  is the refractive index of the gel.<sup>12</sup> <sup>b</sup> First cumulant for 90° scattering with wavelength  $\lambda = 6328$  Å. <sup>c</sup> Variance, where  $\mu_2$  is the second cumulant.

tions in concentration, eq 1, 3, and 4 give for the osmotic compressional modulus at  $c_e$

$$K_{os} = (c\partial\omega/\partial c)|_{c=c_e} = A(s-m)\langle c_e^s \rangle \quad (5)$$

in which the average is taken over the mean polymer concentration raised to the power  $s$ . Intensity measurements from dynamic light scattering, in contrast, yield a longitudinal modulus, formally defined as

$$M_{os} = K_{os} + 4G_s/3 \quad (6)$$

with  $G_s$  the elastic shear modulus. At swelling equilibrium  $G_s$ , like  $G_v$ , is expected to be proportional to  $K_{os}$ . The intensity of the dynamically scattered light then is given by<sup>8</sup>

$$I = kc_e^2(\partial\epsilon/\partial c)^2/M_{os} \quad (7)$$

in which  $k$  is an apparatus constant and  $\epsilon$  the relative permittivity of the scattering medium at the wavelength of the light used.

As the quantity  $\partial\epsilon/\partial c$  hardly depends on  $c$  (cf. Table I), one obtains from eq 7 with only minor error, for the case of a sample containing permanent spatial concentration fluctuations

$$I = k\langle (c_e^2/M_{os}) \rangle (\partial\epsilon/\partial c)^2 \propto \langle c_e^{s'} \rangle \quad (7')$$

where

$$s' = (3\nu - 2)/(3\nu - 1)$$

Thus a measurement of  $M_{os}$  by light scattering involves measuring the normalized intensity of the dynamically scattered light,  $I$ , as well as the average polymer concentration in the sample,  $\langle c_e \rangle$ . The apparent value of  $M_{os}$  from light scattering thus becomes

$$M_{os,light} = k\langle (c_e^2/I) \rangle (\partial\epsilon/\partial c)^2 \propto \langle c_e^2 \rangle / \langle c_e^{s'} \rangle \quad (8)$$

The ratio  $R$  of these two longitudinal osmotic moduli, obtained from osmotic and mechanical techniques, to that obtained from the light scattering observation, is thus, at  $c = c_e$

$$R = (K_{os} + 4G_s/3)/M_{os,light} = \langle c_e^s \rangle \langle c_e^{s'} \rangle / \langle c_e \rangle^2 \quad (9)$$

The assumption is made that the probability distribution  $p(c)$  of the local concentration fluctuations is a Gaussian of width  $\langle \Delta c^2 \rangle$ :

$$p(c) = (2\pi\langle \Delta c^2 \rangle)^{-1/2} \exp[-(c - \langle c_e \rangle)^2/2\langle \Delta c^2 \rangle] \quad (10)$$

where the unphysical negative values of  $c$  have a vanishing probability provided  $\langle \Delta c^2 \rangle / \langle c_e \rangle^2$  is sufficiently small. Expression 9 then becomes in this approximation<sup>1</sup>

$$R = 1 + \frac{1}{(3\nu - 1)^2} \frac{\langle \Delta c^2 \rangle}{\langle c_e \rangle^2} \quad (11)$$

Now the mean-square amplitude  $\langle \Delta c^2 \rangle$  is related to the second moment of the excess small-angle radiation scattering function  $S(Q)$ , where  $Q$ , the scattering wave vector, is given by  $Q = (4\pi n/\lambda) \sin(\theta/2)$ . Here  $n$  is the refractive index (equal to unity for X-rays and neutrons),  $\lambda$  the wavelength of the incident radiation, and  $\theta$  the scattering angle:

$$\langle \Delta c^2 \rangle = \frac{1}{2\pi^2 V(\partial\rho/\partial c)^2} \int_0^{Q_{max}} [S_g(Q) - S_s(Q)] Q^2 dQ \quad (12)$$

where  $V$  is the sample volume and  $\rho$  the electron density.  $(S_g(Q) - S_s(Q))$  is the excess scattering intensity due to the presence of cross-links.  $S_s(Q)$  represents the Lorentzian scattering function of the solution-like regions in the gel, and  $S_g(Q)$  is the total gel scattering function.  $Q_{max}$  ( $\approx 1/\xi$ , where  $\xi$  is the correlation length) is the value of  $Q$  at which these two functions intersect.

Equation 12 is based on the following reasoning. The full second moment of the scattering curve ( $\int S(Q) Q^2 dQ$ , where the upper limit of the integral is infinity) of a given sample is an invariant,<sup>9</sup> depending only on the total number of scattering centers in the sample. Addition of cross-linking agent to the gel is in such a small proportion that the full second moment is unaffected. The shape of the scattering function, however, is altered at low  $Q$  by cross-linking on account of the redistribution of the electron density by the heterogeneities. The truncated second moment of eq 12 provides a measure of how much scattering intensity is transferred from high  $Q$  to low  $Q$  values. This procedure is identical with that used in ref 2. The multiplicative factor appearing in eq 12 is determined by performing static light scattering as a function of angle on the same samples and matching these curves with those from SAXS. Subsequent measurement of the turbidity using a spectrophotometer calibrates the static light scattering curves (and hence the SAXS spectra), so that an absolute estimate is obtained for  $\langle \Delta c^2 \rangle$ .<sup>2</sup> This procedure avoids the difficulty of making absolute intensity measurements in small-angle X-ray scattering.

It is one of the aims of this investigation to examine to what extent the estimates of  $\langle \Delta c^2 \rangle$  from the two above-mentioned approaches are related or compatible.

## Experimental Conditions

Polyacrylamide gels were prepared by copolymerization of 0.08 w/w aqueous solutions of acrylamide (BDH) with five different concentrations (0.001, 0.002, 0.003, 0.004, 0.005 w/w) of  $N,N'$ -methylenebisacrylamide (BDH) at 23 °C. These gels are designated 8/1, 8/2, etc. The precursor solutions were mixed with  $7 \times 10^{-4}$  g/mL ammonium persulfate and  $5.7 \times 10^{-4}$  v/v  $N,N'$ -tetramethylethylenediamine (TEMED). Gelation took place in 10–15 min. The gels were prepared simultaneously in various molds appropriate to the type of experiment to be performed and left for 24 h for the reaction to go to completion. They were then removed from the molds and placed in water baths to achieve swelling equilibrium. Over this period the water was replaced several times to ensure thorough elimination of the sol fraction.

Samples with bisacrylamide concentrations greater than 0.005 w/w display macroscopic syneresis, and the gels become so turbid that dynamic light scattering measurements become impractical.

Each of the experimental techniques used—osmotic deswelling and mechanical measurements<sup>10,11</sup> and dynamic light scattering<sup>12</sup>—has been described in detail elsewhere. The calibration of the dynamic light scattering apparatus was made by using a set of polyacrylamide gels of low cross-linking density, as described in ref 1.

For the small-angle X-ray measurements, rather small samples were necessary. These were made by cutting a 1-mm-thick slice from 5-mm-diameter cylindrical gels and placing it between two thin mica sheets separated by a spacer of appropriate thickness.

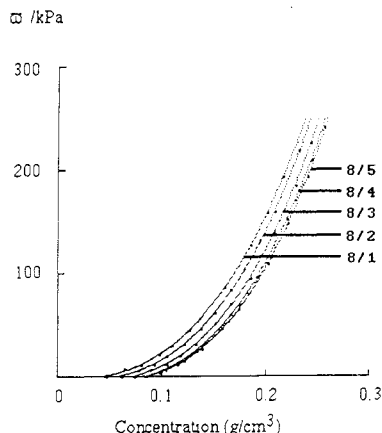


**Figure 1.** Variation of the swelling pressure  $\omega$  as a function of concentration  $c$  for the five polyacrylamide-water gels investigated. The theoretical lines drawn through the points are the fits of the data to the equation  $\omega = A\varphi^s - G_v^*(\varphi/\varphi_0)^m$ , in which  $\varphi = c/\rho_0$ , where  $\rho_0 = 1.3 \text{ g/cm}^3$  is the density of the pure polymer and  $G_v^*$  is listed in Table II.

The mica sheets formed the windows of a stainless steel cell that allowed the sample to bathe in a surrounding reservoir of water, thereby maintaining swelling equilibrium during the course of the experiment.

The SAXS experiments were conducted on the D24 instrument at the LURE laboratory, Orsay, France. A 6-cm linear detector with 256-point resolution was used, and the incident wavelength was 1.608 Å. Sample-detector distances between 0.7 and 2.1 m were chosen. The data were analyzed by subtraction of a background signal from a sample of water of the same thickness as the gel.

## Results

**Dynamic Light Scattering.** The scattering intensity measurements were carried out in the heterodyne mode, at 90° scattering angle with 6328-Å incident wavelength, using dust and heterogeneities in the sample to provide the pseudostatic local oscillator. To remain in the correct quadratic response range of the correlator, low incident light intensities had to be used. This constraint made it increasingly difficult to obtain signals from the most inhomogeneous gels, which displayed strong opalescence, thereby reducing the signal/noise ratio. The proportion of statically scattered light was so large in the most heterogeneous sample (8/5) that it was not possible to extract a meaningful signal.

The results of the dynamic light scattering measurements are listed in Table I, together with the characteristic decay rates

$$\bar{\Gamma} = D_c Q^2 / (1 - \varphi) \quad (13)$$

where  $\varphi = c/\rho_0$  is the volume fraction of the polymer at concentration  $c$ ,  $\rho_0$  is the density of the pure polymer,  $D_c$  is the collective diffusion coefficient, and  $Q$  is the scattering wave vector.<sup>12,13</sup>

**Osmotic Swelling Measurements.** The measured values of the osmotic swelling pressure  $\omega$  are displayed in Figure 1 as a function of gel concentration for the five sets of inhomogeneous gels. The concentration range explored was between  $c_0$  and about 0.25 g/cm<sup>3</sup> at the temperature 25 °C.

The bulk osmotic modulus  $K_{os} = (c\partial\omega/\partial c)|_{c=c_0}$  is obtained from the slope of the best fit through the data of Figure 1 at the equilibrium swelling concentration  $c_0$ , by using eq 3 for the osmotic pressure term II and eq 4 for the elastic term. As can be seen in Table II, the value of the apparent exponent  $s$  in eq 3 rises noticeably as the degree of cross-linking increases, indicating that bisacrylamide lowers

**Table II**  
Fitting Parameters to Swelling Pressure Measurements in Polyacrylamide Gels at 25 °C

sample <sup>a</sup>	$s^b$	$m^b$	$c_0$ (equil concn), g/cm <sup>3</sup>	$G_v^*,^b$ kPa
8/1	2.61	0.38	0.0465	4.0
8/2	2.82	0.26	0.0618	5.8
8/3	2.96	0.33	0.0746	7.3
8/4	2.98	0.40	0.0843	9.8
8/5	3.10	0.35	0.0861	8.4

<sup>a</sup> Samples copolymerized with 0.08 g/cm<sup>3</sup> acrylamide and between 0.001 and 0.005 g/cm<sup>3</sup> bisacrylamide. <sup>b</sup> Apparent power dependence obtained by fitting the data to  $\omega = A\varphi^s - G_v^*(\varphi/\varphi_0)^m$  between the volume fraction of the freely swollen gel,  $\varphi_0$ , and  $\varphi \approx 0.20$ , where  $\varphi = c/\rho_0$ . The density of the dry polymer,  $\rho_0$ , is taken<sup>15</sup> to be 1.3 g/cm<sup>3</sup>.

**Table III**  
Measured Values of Moduli of Polyacrylamide Gels

sample	$G_s^*,^a$ kPa	$G_v^*,^b$ kPa	$K_{os},^c$ kPa	$M_{os},^d$ kPa
8/1	4.86	4.0	7.3	13.9
8/2	9.94	5.8	12.2	24.6
8/3	13.1	7.3	18.3	33.6
8/4	17.2	9.8	26.8	31.2
8/5	17.7	8.4	25.6	

<sup>a</sup> Shear modulus, from uniaxial compression measurements at constant volume. <sup>b</sup> Volume elastic modulus: osmotic deswelling.

<sup>c</sup> Compressional osmotic modulus: osmotic deswelling.

<sup>d</sup> Longitudinal osmotic modulus: dynamic light scattering.

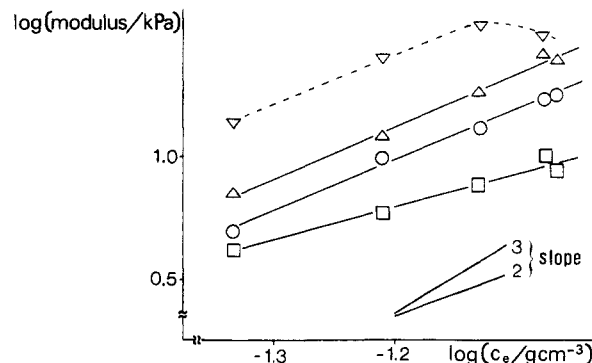


**Figure 2.** Double-logarithmic representation of the various moduli ( $M_{os}$ ,  $\nabla$ ;  $K_{os}$ ,  $\Delta$ ;  $G_s$ ,  $\circ$ ;  $G_v$ ,  $\square$ ) as a function of the swelling equilibrium concentration  $c_0$  for the different polyacrylamide gels investigated.

the solubility of the polymer. The exponent  $m$  describing the concentration dependence of  $G_v$ , however, displays no significant deviation from its theoretical value of  $1/3$ .

The calculated values of  $K_{os}$  and the volume elastic modulus  $G_v^*$  are listed in Table III. Figure 2 shows a double-logarithmic plot of  $K_{os}$  and  $G_v$  as a function of equilibrium swelling concentration.

**Mechanical Measurements.** Measurements of the shear modulus  $G_s$  were made on cylindrical gels using a balance technique.<sup>10,11</sup> Barrel distortion did not occur, and all the curves showed a linear response of force vs  $(\Lambda - 1/\Lambda^2)$ , where  $\Lambda$  is the compression ratio at constant volume along the cylinder axis, in the range  $0.7 \leq \Lambda \leq 1$ .

Values of the resulting moduli  $G_s$  at 25 °C are included in Table III. Contrary to the behavior of lightly cross-linked networks,<sup>1</sup> for the inhomogeneous gels it is apparent that the equilibrium swelling value  $G_s^*$  no longer coincides with  $G_v^*$ .  $G_s^*$  is also displayed in the scaling representation of Figure 2.

In Figure 3 are shown the results of shear modulus measurements on the gels at various degrees of deswelling, up to concentrations in excess of 0.3 g/cm<sup>3</sup>. The slopes

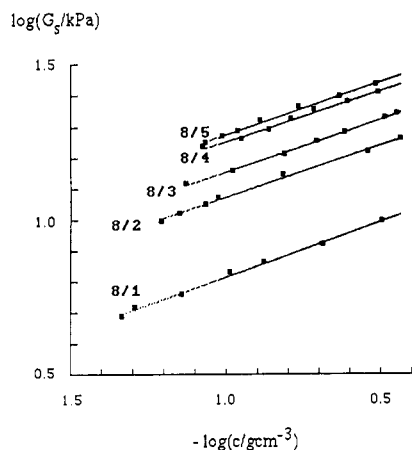


**Figure 3.** Double-logarithmic representation of the shear modulus  $G_s$  as a function of concentration  $c$  during deswelling. The slopes ( $m'$ ) of the straight line fits through each set of points are listed in Table IV.

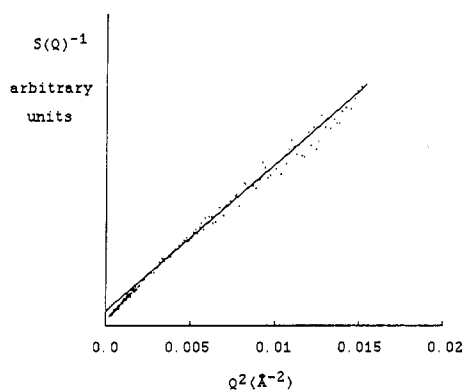


**Figure 4.** Zimm representation of the inverse SAXS scattering intensity as a function of the square of the transfer wave vector,  $Q$  (sample 8/3).

**Table IV**  
Parameters of Least-Square Fits of Shear Modulus Measurements<sup>a</sup> to  $G_s = G_{s0}\varphi^{m'}$

sample	$G_{s0}$ , kPa	$m'$
8/1	16.4	$0.36 \pm 0.01$
8/2	28.1	$0.34 \pm 0.01$
8/3	33.9	$0.34 \pm 0.01$
8/4	40.8	$0.32 \pm 0.01$
8/5	44.3	$0.33 \pm 0.01$

<sup>a</sup> Measurements performed on deswelling in the concentration range  $\varphi_0 \leq \varphi \leq 0.27$ .

of these curves, in a double-logarithmic representation, are in excellent agreement with the theoretically expected<sup>6,7</sup> value of  $1/3$  (cf. Table IV).

**Small-Angle X-ray and Static Light Scattering.** In Figure 4 a typical SAXS spectrum is shown in a Zimm representation. The correlation lengths  $\xi$  extracted from fits of the SAXS spectra to Lorentzians of the form

$$S_s(Q) = B/(1 + Q^2\xi^2) \quad (14)$$

are listed in Table V. While for the less cross-linked samples the separation of the SAXS spectra into two distinct regions, a high- $Q$  homogeneous part (solution-like characteristics) and a low- $Q$  inhomogeneous part, is possible (and consistent with contrast variation observations<sup>2</sup>), this procedure becomes difficult to apply at the highest cross-linking density (sample 8/5), since the signal from the heterogeneous regions extends to high  $Q$  values.

In the calculation of the integral (12), the Lorentzian curves calculated from Figure 4 were used for  $S_s(Q)$ . The

**Table V**  
Comparison between X-ray and Dynamic Light Scattering Results

sample	dynamic light scattering			
	$D_c/10^7$ , cm <sup>2</sup> /s	$\xi_{D_c}$ , <sup>a</sup> Å	$\xi_{M_{90}}$ , <sup>b</sup> Å	$\xi_{X-R}$ , <sup>c</sup>
8/1	6.2	$35 \pm 3$	$41 \pm 2$	$37 \pm 5$
8/2	6.5	$34 \pm 3$	$34 \pm 2$	$34 \pm 3$
8/3	8.0	$27 \pm 2$	$31 \pm 2$	$30 \pm 3$
8/4	6.8	$32 \pm 5$	$31 \pm 3$	$28 \pm 4$

<sup>a</sup> Correlation length calculated from eq 16:  $\xi = kT/(6\pi\eta D_c)$ .

<sup>b</sup> Correlation length calculated from eq 17:  $\xi = (3kT/4\pi M_{90})^{1/3}$ .

<sup>c</sup> Correlation length from fit of SAXS data to eq 14.

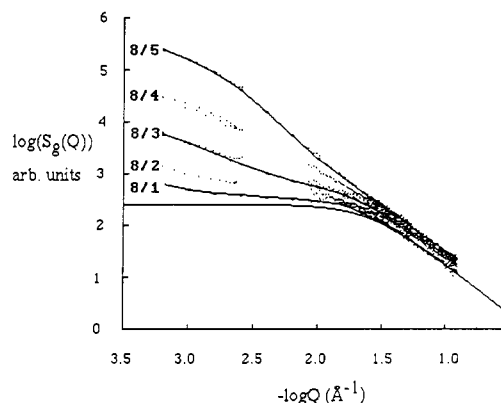


**Figure 5.** Double-logarithmic plot of the combined light scattering and SAXS intensities as a function of scattering wave vector  $Q$ . The Lorentzian fit to the SAXS spectrum of sample 8/1 is shown as the lowest continuous line in the figure. The three higher continuous lines represent the interpolations for samples 8/1, 8/3, and 8/5, used to calculate the excess second moment (eq 12) and the turbidity (eq 15) of the spectra.

error involved in this approximation is small, since the good solvent  $Q^{-5/3}$  scattering behavior begins beyond  $Q_{\max} \approx 1/\xi$ , where  $\xi$  is the polymer-polymer correlation length in the solution.<sup>4</sup>

In Figure 5 the combined intensity measurements from SAXS and static light scattering (SLS) are plotted in a double-logarithmic representation. This plot allows the constant multiplicative factors in the scattered intensity, which arise when the incident wavelength changes between different sets of data (e.g., on going from X-ray to visible light), to be corrected for by sliding one set of curves  $S(Q)$  with respect to the other parallel to the intensity axis, to achieve suitable continuity. In the present case, the lowest SAXS transfer wave vectors did not overlap with the highest values in the SLS measurements (488 nm), but it is possible to obtain a reasonable fit by interpolation between the two sets of curves. The SLS measurements were made at 546 and 488 nm. In practice, the values of  $\langle \Delta c^2 \rangle$  calculated from the curves of Figure 5 are fairly insensitive to the uncertainty introduced by the fitting procedure, since the overwhelming contribution to the second moment (12) arises in the transfer wave vector region just below  $Q_{\max}$ .

From the set of curves shown in Figure 5, the following light scattering integral can be calculated:

$$M_0 = \int_0^\pi S_g(\theta) \sin \theta (1 + \cos^2 \theta) \pi d\theta \quad (15)$$

in which  $\theta$  and  $Q$  are related, as before, by

$$Q = (4\pi n/\lambda) \sin(\theta/2) \quad (16)$$

where the wavelength of the incident light  $\lambda$  is 488 nm and the refractive index of the gel medium,  $n$ , is about 1.34.

The integral  $M_0$  is simply equal to the optical turbidity  $\tau$  of the sample at the wavelength  $\lambda$ . The numerical factor

Table VI  
Comparison of SAXS Results with Dynamic Light Scattering and Macroscopic Measurements

sample	$\nu_{\text{app}} = s/3(s-1)$	$\langle \Delta c^2 \rangle / 10^3, \text{ g}^2/\text{cm}^6$	$\langle \Delta c^2 \rangle / (3\nu - 1)^2 \langle c_e \rangle^2$	$R = (K_{\text{os}} + 4G_s/3)/M_{\text{os}}$
8/1	0.540	0.11	0.13	$0.99 \pm 0.1$
8/2	0.516	0.16	0.14	$1.04 \pm 0.1$
8/3	0.504	0.67	0.46	$1.07 \pm 0.1$
8/4	0.501	1.5	0.85	$1.6 \pm 0.2$
8/5	0.492	3.0	1.8	

$\pi$  rather than  $2\pi$  appearing in eq 11 is the result of the fact that the scattering function  $S(Q)$  is defined for incident light that is vertically polarized with respect to the scattering plane. Measurement of  $\tau$  for one or more of the samples at the same wavelength as the chosen SLS reference measurements (546 nm) thus provides a calibration for all the radiation scattering data shown in Figure 5. This was accomplished by using the most turbid sample (8/5), for which the optical density of a 1-cm thickness was found to be 0.61 at  $\lambda = 546$  nm, giving  $\tau = 1.41 \text{ cm}^{-1}$  at this wavelength. For this sample and wavelength, integration of expression 15 using the data of Figure 5 gives  $M_0 = 6.0 \times 10^5$  in the intensity units of that figure.

In the calculation of  $\langle \Delta c^2 \rangle$  from expression 12, the value of  $V$  is irrelevant on account of the normalization procedure described above, whereby scattering intensities are defined in terms of an absolute measurement, the optical turbidity.  $V$  can therefore be taken as unity. A further consequence of this procedure is that the factor  $(\partial \rho / \partial c)^2$  appearing in (12) must be replaced by  $(\partial \epsilon / \partial c)^2$  from light scattering. The values of  $\langle \Delta c^2 \rangle$  calculated from Figure 5 are listed in Table VI.

## Discussion

The results of this investigation, summarized in Tables I–VI, supply new information on the properties of swollen heterogeneous polyacrylamide gels.

For the dynamic light scattering results, it can be seen from column 4 of Table I that the variance of the spectra remains small ( $<0.1$ ) for all the samples. This implies a narrow distribution of correlation times and is in agreement with previous observations which indicated that these gels contain extensive regions that can be characterized by the same correlation length.<sup>2</sup>

A further result of these measurements, visible in Table V, is that the dynamic correlation lengths  $\xi_{D_c}$  calculated from the scaling relation<sup>4</sup>

$$D_c = kT / (6\pi\eta\xi) \quad (17)$$

in which  $\eta$  is the viscosity of water, are in agreement, in both magnitude and direction of trend, with those of SAXS. Still another estimate of the correlation length can be obtained from the intensity of the dynamic light scattering,<sup>12</sup> which yields

$$M_{\text{os}} = 3kT / 4\pi\xi^3 \quad (18)$$

The results of this calculation, displayed in column 4 of Table V, are also consistent with the other two estimates.

The osmotic swelling results in Table II show that increasing the cross-linking density with bisacrylamide substantially modifies the osmotic component  $\Pi$  in the swelling pressure. The variation of the exponent  $s$  indicates a crossover from good solvent to  $\Theta$  condition. Moreover, as the solvent power of the diluent falls, an increasingly inhomogeneous network structure develops. One obvious reason for this trend is that inclusion of relatively insoluble bisacrylamide in the acrylamide chains increases the repulsive potential between polymer and the solvent. A second, less direct, contribution arises from the

restriction in degrees of liberty due to the cross-links: as the local polymer concentration is no longer  $\langle c \rangle$ , the effective polymer-solvent interaction is necessarily modified from its value in an un-cross-linked solution. From this investigation it is not possible to discriminate between either of these effects.

The dependence of the moduli  $K_{\text{os}}$ ,  $G_v$ , and  $G_s$  upon the swelling equilibrium concentration,  $c_e$ , is displayed in a double-logarithmic representation in Figure 2. The observed variation is weaker (exponent  $\leq 2$ ) than that expected from the exponents  $s$  in the deswelling experiments. This behavior differs from that of homogeneous polyacrylamide gels, where the slopes of  $K_{\text{os}}(c_e)$  and  $G_v(c_e)$  and the exponent  $s$  were found to be mutually consistent.<sup>1</sup> Another notable distinction from homogeneous gels is the difference between the shear and volume moduli,  $G_s^e$  and  $G_v^e$  (Table III). The ratio  $G_s^e/G_v^e$  increases with increasing bisacrylamide content, reaching the value 2 for the most heterogeneous sample. The variation of both moduli upon deswelling, however, is consistent with a one-third power law concentration dependence (cf. Table II, column 3, and Table IV, column 3).

We now turn to the combination of dynamic light scattering and osmotic data. From the values of  $K_{\text{os}}$ ,  $G_s$ , and  $M_{\text{os}}$  listed in Table III the ratio  $R = (K_{\text{os}} + 4G_s/3)/M_{\text{os}}$  of the longitudinal modulus obtained from the mechanical and osmotic swelling measurements to that of dynamic light scattering can be calculated. The results, listed in the last column of Table VI, indicate that  $R$  increases with increasing bisacrylamide content. For the most homogeneous sample, the value of  $R$  is close to unity, while in the case of the heterogeneous sample, it is 1.6. This finding underlines the fact that the two kinds of experiment measure different concentration averages arising from the heterogeneities.

The mean-square fluctuation in concentration  $\langle \Delta c^2 \rangle$ , calculated from the SAXS spectra, is also listed in Table VI. This quantity shows a strong increase with increasing bisacrylamide content, suggesting an approaching partial phase separation.  $\langle \Delta c^2 \rangle$  can alternatively be viewed as strongly varying with  $c_e$ , but its dependence is not described by a simple function. With the exception of sample 8/1, the values of  $\langle \Delta c^2 \rangle$  found here are somewhat larger than but of the same order of magnitude as those reported for similar gels at the concentration of network formation.<sup>2</sup> Sample 8/1 distinguishes itself by a value of  $\langle \Delta c^2 \rangle$  some 4 times larger than its unswollen counterpart. Although allowance should be made for variability between samples prepared in the same way, this discrepancy is possibly the result of differential swelling between more and less densely cross-linked regions in the sample.<sup>14</sup>

The parameter  $R$  can be compared with the quantity  $1 + \langle \Delta c^2 \rangle / \{(3\nu - 1)\langle c_e \rangle\}^2$ , obtained from SAXS. The results are displayed in Table VI. It should be stressed that for sample 8/4 and 8/5 the condition  $(\langle \Delta c^2 \rangle / \langle c_e \rangle^2) \ll 1$  is not obeyed, so that the Gaussian distribution (eq 10) for the concentration fluctuations can at best be considered only to be a rough approximation. In view of the experimental uncertainties, the agreement appears to be satisfactory. The principal source of experimental error in this comparison lies undoubtedly in the dynamic light scattering evaluation of  $M_{\text{os}}$ .

## Conclusions

A set of heterogeneous acrylamide-bisacrylamide copolymer networks swollen in water was investigated by using a variety of complementary experimental techniques. The gels were all prepared at the same acrylamide concentration, with differing bisacrylamide content.

The principal results are as follows:

For lightly cross-linked gels, the longitudinal osmotic modulus  $M_{os}$  determined by osmotic and mechanical measurements is in accord with that obtained from dynamic light scattering. The ratio  $R$  of these two quantities increases as the gel heterogeneities increase.

SAXS measurements of the mean-square concentration fluctuations ( $\Delta c^2$ ) associated with the heterogeneities in the fully swollen gels are in reasonable quantitative agreement with that deduced from the ratio  $R$ . The values of  $\langle \Delta c^2 \rangle$  increase strongly with increasing cross-link content.

Estimates of the correlation length from three independent measurement techniques, namely, SAXS, dynamic light scattering intensity, and collective diffusion measurements, yield values that are consistent with one another.

Over the concentration range studied, the shear and volume elastic moduli both follow a one-third power dependence as a function of the concentration  $c$ , even for the most heterogeneous sample, but their numerical values diverge from each other as the cross-linking density increases.

**Acknowledgment.** We thank J. P. Benoit for his valuable help and advice in the SAXS experiments and the Laboratoire pour l'Utilisation du Rayonnement Electromagnetique (L.U.R.E.) for granting beam time.

This work received support from a joint CNRS-Hungarian Academy of Sciences project. We also acknowledge the Hungarian Academy of Sciences for research contract AKA No. 1-36-86-229.

**Registry No.** (Acrylamide)( $N,N'$ -methylenebisacrylamide) (copolymer), 25034-58-6.

## References and Notes

- (1) Geissler, E.; Horkay, F.; Hecht, A. M.; Zrinyi, M. *Macromolecules* **1988**, *21*, 2594.
- (2) Hecht, A.-M.; Duplessix, R.; Geissler, E. *Macromolecules* **1985**, *18*, 2167.
- (3) Flory, P. J. *Principles of Polymer Chemistry*; Cornell University Press: Ithaca, NY, 1953.
- (4) de Gennes, P.-G. *Scaling Concepts in Polymer Physics*; Cornell University Press: Ithaca, NY, 1979.
- (5) Muthukumar, M. *J. Chem. Phys.* **1986**, *85*, 4722.
- (6) James, H. M.; Guth, E. J. *J. Chem. Phys.* **1943**, *11*, 455.
- (7) Treloar, L. R. G. *The Physics of Rubber Elasticity*; Oxford University Press: Oxford, 1975.
- (8) Tanaka, T.; Hocker, L. O.; Benedek, G. B. *J. Chem. Phys.* **1973**, *59*, 5151.
- (9) Glatter, O.; Kratky, O. *Small Angle X-Ray Scattering*; Academic Press: London, 1982.
- (10) Nagy, M.; Horkay, F. *Acta Chim. Acad. Sci. Hung.* **1980**, *104*, 49.
- (11) Horkay, F.; Zrinyi, M. *Macromolecules* **1982**, *15*, 1306.
- (12) Geissler, E.; Hecht, A. M. *J. Phys. (Les Ulis, Fr.)* **1978**, *39*, 955.
- (13) Geissler, E.; Hecht, A. M. *J. Phys. (Les Ulis, Fr.)* **1979**, *40*, L-173.
- (14) Bastide, J.; Leibler, L. *Macromolecules* **1988**, *21*, 2648.
- (15) Scholtan, W. *Macromol. Chem.* **1954**, *14*, 169.

## Gels of Rigid Polyamide Networks

**S. M. Aharoni\***

*Engineered Materials Sector, Allied-Signal Inc., Morristown, New Jersey 07960*

**S. F. Edwards**

*Cavendish Laboratory, Cambridge University, Madingley Rd., Cambridge CB3 0HE, U.K.  
Received December 2, 1988; Revised Manuscript Received January 24, 1989*

**ABSTRACT:** Gels were prepared comprising highly branched networks of rigid rodlike segments and a good solvent. Several networks in which some flexibility was built into the chain were prepared for comparison. All these systems show a remarkably steep approach to the gel point and large viscosity increases beyond it. Fractionation and end-group titrations show that the higher the rigidity of the network the less sol is extractable and the lower its molecular weight, indicating that due to segmental rigidity, individual highly branched macromolecules can hardly diffuse out of the "infinite" network, while more flexible macromolecules diffuse out with greater facility. The modulus of the gels increases with increased network concentration. This holds for gels equilibrated and immersed during measurements in good as well as in poor solvent. The modulus of the equilibrated immersed rigid networks appears to be insensitive to temperature changes over the range 23–150 °C. In networks with more flexibility, the modulus of the immersed gels drops with temperature, and the drop appears to be associated with increased swelling of the gels. It seems that the segments between branch points, even those termed "flexible" in this study, are far too short and too rigid to conform with Gaussian statistics and for the gels to behave accordingly. A schematic description of the rigid network structures is proposed.

## Introduction

In the term "gel" are included such disparate systems as lamellar mesophases, inorganic clays, vanadium pentoxide gels, phospholipids, certain disordered proteins, and, of course, three-dimensional or network polymers.<sup>1</sup> Polymeric gels are capable, in general, of absorbing large amounts of solvent and, like all other gels, exhibit properties of solids such as modulus and shape retention. In this paper we describe a new class of network polymeric gels with remarkable properties. For the purpose of this work we define polymeric gel as a system consisting of a

polymer network swollen with solvent and a polymer network as a three-dimensional polymeric structure excluding the occluded solvent. The polymeric gels may be categorized in two major classes: thermoreversible gels and permanent gels. The thermoreversible gels undergo a transition from an immobile gel below a certain characteristic temperature, to a spontaneously flowing solution above it. The links between the polymeric chains are transient in nature and support a stable polymeric network only below the characteristic "melting" point. Prominent among such links are polymer-polymer and polymer-